V European Conference on Computational Fluid Dynamics
ECCOMAS CFD 2010
J. C. F. Pereira and A. Sequeira (Eds)
Lisbon, Portugal, 14–17 June 2010

A DIFFUSION-INERTIA MODEL (DIM) FOR PREDICTING AEROSOL TRANSPORTATION AND DEPOSITION IN TURBULENT FLOWS

R.V. Mukin, L.I. Zaichik, and L.S. Mukina

Nuclear Safety Institute of the Russian Academy of Sciences
Bolshaya Tulskaya 52, Moscow, Russia, 115191
e-mail: mukin@ibrae.ac.ru

Key words: Particle-laden turbulent flow, particle deposition, monodisperse aerosols, bend

Abstract. *The model presented in the paper is based on a kinetic equation for the probability density function (PDF) of particle velocity distribution [1, 2]. In comparison with the latter, the DIM allows us to take into account a number of effects caused by the particle inertia: (i) the impact of gravity and other body forces, (ii) the so-called inertial bias effect, i.e., the transport by reason of the deviation of particle trajectories from the fluid streamlines, (iii) the preferential accumulation of particles due to turbophoresis, and (iv) the inertia and crossing-trajectory effects on particle turbulent diffusivity. As the boundary condition for the particle concentration equation, we invoke a relation between the flow rate of depositing particles and the particle concentration in the near-wall region. The DIM was incorporated in a finite-volume CFD code and coupled with fluid RANS in the frame of two-way coupling. The fluid turbulence is simulated using a nonlinear, explicit algebraic Reynolds model, along with the two-equation* $k-\varepsilon$ *model with taking into account particles influence on turbulence. The DIM was applied to simulations of aerosol dispersion and deposition in isothermal and non-isothermal turbulent flows inside straight ducts and circular bends, when the transport of particles is caused by the action of diffusion, thermophoresis, turbophoresis, and centrifugal force. The predictions of deposition efficiency obtained using the DIM were found to be in encouraging agreement with available experimental data and Lagrangian tracking simulations coupled with fluid DNS or LES.*

INTRODUCTION

The existing strategies of modeling turbulent two-phase flows can be subdivided into two groups depending on the Lagrangian tracking and Eulerian continuum approaches for handling the particulate phase. In the framework of the Lagrangian method, the particles are assumed to encounter randomly a series of turbulent eddies, and the macroscopic particle properties are determined solving stochastic equations along separate trajectories. As a consequence, such a method requires tracking a very large number of particle trajectories to achieve statistically invariant solution. As the size of particles decreases, the representative number of realizations should increase because of the increasing contribution of particle interactions with turbulent eddies of smaller and smaller scale. Thus, this technique, especially when coupling with DNS or LES for the computation of fluid turbulence, provides a very useful research tool of investigating particle-laden flows, but it can be too expensive for engineering calculations. The Eulerian method deals with the particulate phase in much the same manner as with the carrier fluid phase. Therefore, the two-fluid modeling technique is computationally very efficient, as it allows us to use the governing equations of the same type for both phases. In addition, the description of fine particles does not cause great difficulties because the problem of the transport of particles with vanishing response times reduces to the turbulent diffusion of a passive impurity. Overall, the Lagrangian tracking and Eulerian continuum modeling methods complement each other. Each method has its advantages and, consequently, its own field of application.

To simulate the dispersion of low-inertia particles in turbulent flows, the Eulerian models of diffusion type appear to be very efficient. In [4-6], a simplified Eulerian model called the diffusion-inertia model (DIM) was developed. This model was based on a kinetic equation for the probability density function (PDF) of particle velocity distribution [1-3] and was coupled with fluid RANS in the frame of two-way coupling.

1 MATHEMATICAL FORMULATION

1.1 Diffusion-Inertia Model (DIM)

The governing equation for the concentration of low-inertia particles is given by [7]:

$$\frac{\partial \Phi}{\partial t}+\frac{\partial U_i \Phi}{\partial x_i}+\frac{\partial}{\partial x_i}\left[\tau_p\left(F_i-\frac{DU_i}{Dt}\right)\Phi\right]=\frac{\partial}{\partial x_i}\left[\frac{\partial D_B \Phi}{\partial x_i}+D_{Tp\,ij}\frac{\partial \Phi}{\partial x_j}+\tau_p \Phi \frac{\partial\left(\langle u_i' u_k'\rangle f_{u\,kj}\right)}{\partial x_j}\right] \quad (1)$$

By this means, for low-inertia particles, namely, when the particle response time is shorter than the turbulence time macroscale, the conservation equation set is reduced to the diffusion-type equation for the particle concentration, and hence one does not require solution to conservation equations for the momentum of the particulate phase. This approach is called the diffusion-inertia model (DIM). In the limit of zero-inertia particles ($\tau_p \to 0$), Eq. (1) becomes the conventional diffusion equation:

$$\frac{\partial \Phi}{\partial t}+\frac{\partial U_i \Phi}{\partial x_i}=\frac{\partial}{\partial x_i}\left(D_B\frac{\partial \Phi}{\partial x_i}+D_{T\,ij}\frac{\partial \Phi}{\partial x_j}\right),\ D_{T\,ij}=\langle u_i' u_j'\rangle T_L \quad (2)$$

with $D_{T\,ij}$ being the diffusion tensor of noninertial admixture.

In comparison with (2), Eq. (1) allows us to take into account a number of effects caused by the particle inertia: (i) the impact of gravity and other body forces, (ii) the so-called inertial bias effect, i.e., the transport by reason of the deviation of particle trajectories from the fluid streamlines, (iii) the turbulent migration (turbophoresis) due

to the gradients of velocity fluctuations, and (iv) the inertia and crossing-trajectory effects on particle turbulent diffusivity.

The response time of aerosol particles is given by

$$\tau_p = \tau_{p0}\left\{1+\mathrm{Kn}\left[A_1 + A_2\exp\left(-\frac{A_3}{\mathrm{Kn}}\right)\right]\right\}\left(1+0.15\,\mathrm{Re}_p^{0.687}\right)^{-1},\ \tau_{p0} = \frac{\rho_p d_p^2}{18\rho_f \nu_f}, \tag{3}$$

where according to [8] $A_1 = 1.20$, $A_2 = 0.41$, and $A_3 = 0.88$. The particle Reynolds number appearing in (3) is evaluated as

$$\mathrm{Re}_p = \frac{d_p\left[|\mathbf{V}_r|^2 + 2\left(1-2f_u^m\right)k\right]^{1/2}}{\nu_f},\ f_u^m = \frac{f_u^l + 2f_u^n}{3}.$$

The Brownian diffusivity is equal to

$$D_B = \frac{k_B T}{3\pi\rho_f \nu_f d_p}\left\{1+\mathrm{Kn}\left[A_1 + A_2\exp\left(-\frac{A_3}{\mathrm{Kn}}\right)\right]\right\}.$$

In a quasi-isotropic approximation that corresponds to averaging over different directions, Eq. (1) and the relative velocity $\mathbf{V}_r$ can be presented as

$$\frac{\partial\Phi}{\partial t} + \frac{\partial U_i\Phi}{\partial x_i} + \frac{\partial}{\partial x_i}\left[\tau_p\left(F_i - \frac{DU_i}{Dt}\right)\Phi\right] = \frac{\partial}{\partial x_i}\left[\left(D_B + D_{Tp}^m\right)\frac{\partial\Phi}{\partial x_i}\right] + \frac{\partial}{\partial x_i}\left(\Phi\frac{\partial q_u^m D_{Tp}^m}{\partial x_i}\right), \tag{4}$$

$$V_{r\,i} = V_i - U_{p\,i} = \tau_p\left(F_i + \frac{DU_i}{Dt}\right) - \frac{1}{\Phi}\frac{\partial}{\partial x_i}\left[\left(D_B + q_u^m D_{Tp}^m\right)\Phi\right], \tag{5}$$

$$D_{Tp}^m = \frac{D_T T_{Lp}^m}{T_L},\ D_T = \frac{\nu_T}{\mathrm{Sc}_T},\ T_{Lp}^m = \frac{T_{Lp}^l + 2T_{Lp}^n}{3},\ q_u^m = \frac{q_u^l + 2q_u^n}{3},\ q_u^\varsigma = \frac{\tau_p f_u^\varsigma}{T_{Lp}^\varsigma}.$$

Note that, in (4) as compared to (1), the space dependence of the Brownian diffusivity is ignored.

Solution to Eq. (1) or (4) right up to the wall is made difficult by the fact that the concentration of particles can steeply rise due to turbophoresis in near wall region. In order to avoid the need to solve the particle concentration equation up to the wall, we use the method of wall-functions that has extensively employed starting from [9] in modeling single-phase turbulent flows. In accordance with the wall-function method, we invoke, as the boundary condition, a relation between the flow rate of deposing particles J_w and the particle concentration in the near-wall region outside the viscous sub-layer Φ_1

$$J_w = \frac{1-\chi}{1+\chi}\left(\gamma V_{DT} + V_{CF}\right)\Phi_1, \tag{6}$$

$$V_{DT} = V_{DF} + V_{TR},\ V_{CF} = U_w + \tau_p\left(F_w - \left.\frac{DU}{Dt}\right|_w\right),\ \gamma = \frac{\exp\left(-b^2/\pi\right)}{1+\mathrm{erf}\left(b/\pi^{1/2}\right)},\ b = \frac{V_{CF}}{V_{DT}}.$$

Here V_{DT} designates the ‘diffusion–turbulence’ component of the particle deposition rate caused by diffusion V_{DF} and turbophoresis V_{TR}. The quantity V_{CF} designates the

'convection–force' component of the deposition rate induced by an action of convection and body forces in the near-wall region, where U_w, F_w, and $DU/Dt\big|_w$ are the normal-wall components of fluid velocity, body force acceleration, and fluid acceleration in the near-wall region. The rebound coefficient, χ, measures a probability of the rebound of a particle from the wall and its return into the flow after collision. The surface is perfectly adsorbing if $\chi = 0$, and the particle deposition is absent if $\chi = 1$. The parameter b quantifies the ratio of the 'convection–force' and 'diffusion–turbulence' components of the deposition rate. Deposition is controled by the 'convection–force' mechanism when $b \to \infty$ ($\gamma \to 0$), and the deposition rate tends to zero when $b \to -\infty$ ($\gamma \to -b$) because the action of this inhibits the motion of particles to the wall. The deduction of the coefficient γ, and relations for particle deposition rates V_{DF}, V_{TR} and V_{CF} is given in [7].

The boundary condition (6) is valid for the particles with $\tau_+ \equiv \tau_{p0} u_*^2 / \nu_f \le 100$ when the first grid node is chosen outside the viscous sub-layer, where Φ_1 changes weakly with variation in the normal distance from the wall.

1.2 Continuous phase

In what follows let us consider the governing equations for the carrier fluid. When the volume fraction of the particulate phase is small ($\Phi \ll 1$), its effect on the continuity equation of incompressible fluid is negligible and this is written as

$$\frac{\partial U_i}{\partial x_i} = 0 \tag{8}$$

The balance fluid momentum equation is given by:

$$\frac{DU_i}{Dt} = -\frac{1}{\rho_f}\frac{\partial \mathrm{P}}{\partial x_i} + \frac{\partial}{\partial x_j}\left(\nu_f \frac{\partial U_i}{\partial x_j} - \langle u_i' u_j' \rangle\right) + A_i, \tag{9}$$

$$A_i = \frac{\rho_p}{\rho_f \tau_p}\int \langle (v_i - u_i) p \rangle d\mathbf{v} = \frac{M}{\tau_p}\left(V_i - U_{p\,i}\right),$$

where $M \equiv \rho_p \Phi / \rho_f$ is the mass particle loading of the fluid, and A_i quantifies the back-effect of particles on the fluid momentum that is determined using (5).

1.3 Turbulence model

Turbulent flow characteristics are simulated on the basis of a two-equation turbulence model incorporating the equations of kinetic turbulence energy and its dissipation, that is, the $k-\varepsilon$ turbulence model. In the frame of this model, the fluid kinetic stresses are given by [7]:

$$\langle u_i' u_j' \rangle = \frac{2k\delta_{ij}}{3} - \nu_T\left(\frac{\partial U_i}{\partial x_j} + \frac{\partial U_j}{\partial x_i} - \frac{2}{3}\frac{\partial U_k}{\partial x_k}\delta_{ij}\right), \tag{10}$$

$$\nu_T = \frac{C_\mu \left(1 + Mf_{u1}\right) k^2}{\varepsilon_m + \left(\Pi_m - \varepsilon_m\right)/C_1},\ C_\mu = \frac{2\left(1 - C_2\right)}{3C_1},\ \varepsilon_m = \varepsilon + \frac{2M}{\tau_p}\left(1 - f_u^m\right)k,$$
$$\Pi_m = \left(1 + Mf_{u1}^m\right)\Pi.$$

It is clear from (10) that, as distinct from the turbulent viscosity coefficient of the standard $k-\varepsilon$ model $\nu_{T0} = C_\mu k^2/\varepsilon$, ν_T incorporates two additional effects: (i) the presence of particles in the flow and (ii) the non-equilibrium of turbulence that lies in a possible inequality between the production and the dissipation. If the particles are absent ($M = 0$, $\Pi_m = \Pi$, $\varepsilon_m = \varepsilon$) and the equilibrium between the processes of production and dissipation takes place ($\Pi = \varepsilon$), ν_T reduces to ν_{T0}. In the equilibrium approach ($\Pi_m = \varepsilon_m$) which is valid, for example, for modelling the turbulent near-wall flow, (10) predicts

$$\nu_T = \frac{C_\mu \left(1 + Mf_{u1}\right) k^2}{\varepsilon + \varepsilon_p}.$$

The turbulence energy balance equation is conclusively given as

$$\left(1 + Mf_{u1}\right)\frac{Dk}{Dt} = \frac{\partial}{\partial x_i}\left\{\left[\nu_f + \left(1 + Mf_{u1}\right)\frac{\nu_T}{\sigma_k}\right]\frac{\partial k}{\partial x_i}\right\} + \left(1 + Mf_{u1}\right)\Pi - \left(\varepsilon + \varepsilon_p + G_p\right) \qquad (11)$$

By analogy with (11), the turbulence dissipation balance equation is represented in the form

$$\left(1 + Mf_{u1}\right)\frac{D\varepsilon}{Dt} = \frac{\partial}{\partial x_i}\left\{\left[\nu_f + \left(1 + Mf_{u1}\right)\frac{\nu_T}{\sigma_\varepsilon}\right]\frac{\partial \varepsilon}{\partial x_i}\right\} + \frac{\varepsilon}{k}\left[C_{\varepsilon 1}\left(1 + Mf_{u1}\right)\Pi - C_{\varepsilon 2}\left(\varepsilon + \varepsilon_p + G_p\right)\right] \qquad (12)$$

By this means, the standard $k-\varepsilon$ model is modified in two aspects. Firstly, the modulation of turbulence due to particles is taken into consideration. Secondly, instead of standard expression for the eddy viscosity coefficient, ν_T is assumed to be a function of the turbulence production-to-dissipation ratio Π_m/ε_m. The values of constants in (10)–(12) are usually taken to be as follows: $C_\mu = 0.09$, $\sigma_k = 1.0$, $\sigma_\varepsilon = 1.3$, $C_{\varepsilon 1} = 1.44$, $C_{\varepsilon 2} = 1.92$. Moreover, $C_1 = 1.1$, $\mathrm{Sc}_T = 0.9$, and $\alpha = C_\mu^{1/2} = 0.3$.

2 RESULTS

The DIM, consisting of the particle concentration equation (4) and the boundary condition (6), is coupled with the fluid balance equations (8), (9), (11), and (12). The model advanced is evaluated against experiments and numerical simulations of aerosol deposition in straight ducts and circular bends. The surface is assumed to be perfectly adsorbing, that is, the rebound coefficient χ is taken as zero in (6). Calculations have been performed using a three-dimensional finite-volume CFD code OpenFOAM.

2.1 Aerosol deposition in straight ducts

First we examine the performance of the model for the deposition of particles in a vertical duct flow, when the gravity force does not exert direct action on the deposition rate. It is a common convention to describe the deposition rate of particles from

turbulent flow by the dependence of the deposition coefficient $j_+ \equiv J_w / \Phi_m u_*$, where Φ_m is the bulk volume particle fraction, on the particle inertia parameter τ_+. In line with the primary mechanism governing the process of deposition, the entire range of particle inertia may be subdivided into three regimes: the diffusion regime ($\tau_+ < 1$), the turbophoresis regime ($1 \le \tau_+ \le 100$), and the inertia regime ($\tau_+ > 100$). The deposition process of the diffusion regime is mainly governed by Brownian and turbulent diffusion. In addition, some driving forces that cause transport of submicron particles (e.g., thermophoresis in non-isothermal flow) can play a significant role. In the situation when the diffusion mechanism plays the leading role, j_+ declines monotonously with τ_+ as a result of a decrease in the Brownian diffusivity as the aerosol size increases. The basis deposition mechanism of the turbophoresis regime is the turbulent migration of particles from the flow core, which is characterized by high-level velocity fluctuation intensity, to the viscous sublayer adjacent the wall. This regime features a strong dependence of j_+ on τ_+. Kallio and Reeks [10] and McLaughlin [11] were the first to establish numerically the tendency of deposing particles to accumulate in the viscous sub-layer under the action of turbophoresis; this effect was reproduced in numerous later works. High-inertia particles ($\tau_+ > 100$) are weakly involved in turbulent flow of the carrier fluid, which causes the deposition coefficient j_+ in a vertical duct to decrease with τ_+.

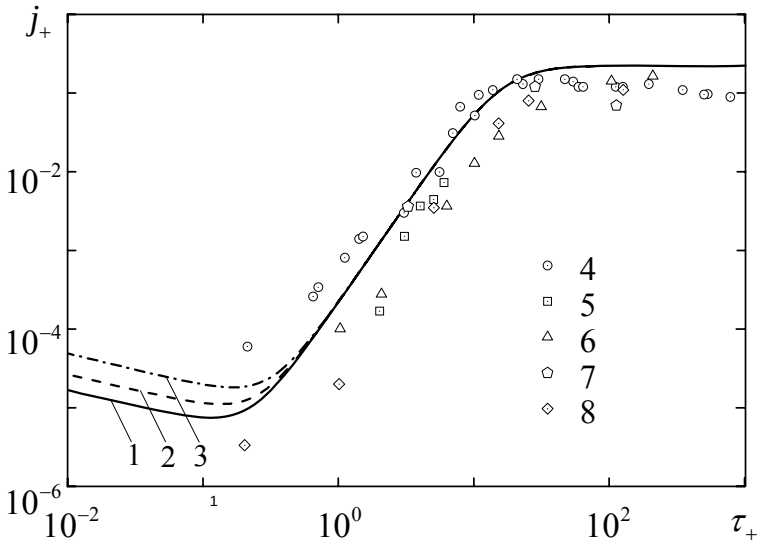

Figure 1: The deposition coefficient in vertical duct flows. (1-3) DIM: (1) Re = 10000, (2) Re = 20000, (3) Re = 50000, (4) experiment by Liu and Agarwal [12], (5) DNS by McLaughlin [11], (6) LES by Wang et al. [15], (7) DNS by Marchioli et al. [13], (8) DNS by Marchioli et al. [14].

Fig. 1 presents the predictions of the deposition coefficient for the pipe flow conditions which correspond to experiments by Liu and Agarwal [12]. To focus attention on the deposition mechanisms caused by the interaction of particles with turbulent eddies, the gravity and lift forces are neglected and hence $F_i = F_w = 0$. In Fig. 1, the deposition coefficients obtained for duct flows using DNS [11, 13, 14] and LES [15] are shown as well. Note that, in the diffusion and turbohoresis regimes, the deposition process is mainly governed by the interaction of particles with near-wall

turbulent eddies. Therefore, the deposition rates determined in round pipe and flat channel flows are hardly distinguishable. As is clear from Fig. 1, the DIM properly captures the dependence of j_+ on τ_+ at $\tau_+ < 100$. The deposition coefficient predicted for high-inertia particles is found to systematically deviates from the measurements, because the model does not predicts a decrease in j_+ with τ_+. Thus, the DIM can be successfully employed in predicting the deposition rate in the diffusion and turbophoresis regimes.

2.2 Continuous flow field in circular bends

In what follows we focus our attention on the deposition of aerosol particles in bends. Hydrodynamic structure of these flows is complex. It is characterized by the existence of curved streamlines and recirculating regions. The key nondimensional parameters that govern the flow are the Reynolds number defined as $\mathrm{Re} = DU_m / \nu_f$ and the Dean number defined as $\mathrm{De} = \mathrm{Re} / R_0^{1/2}$ where $R_0 \equiv 2R_b / D$ is the curvature ratio. For high Dean numbers, the flow in the bend is mainly governed by the centrifugal force which changes cardinally the flow pattern as compared to that in the straight duct. Fig. 2 show, respectively, the streamlines of the mean flow in the midplane and the streamlines of the secondary flow for the deflection angle of 90°. The main features of the flow in the bend consist in separating the mean flow from the inner side, displacing it to the outer side, and generating the secondary flow in the form of a symmetric pair of counter-rotating helical vortices.

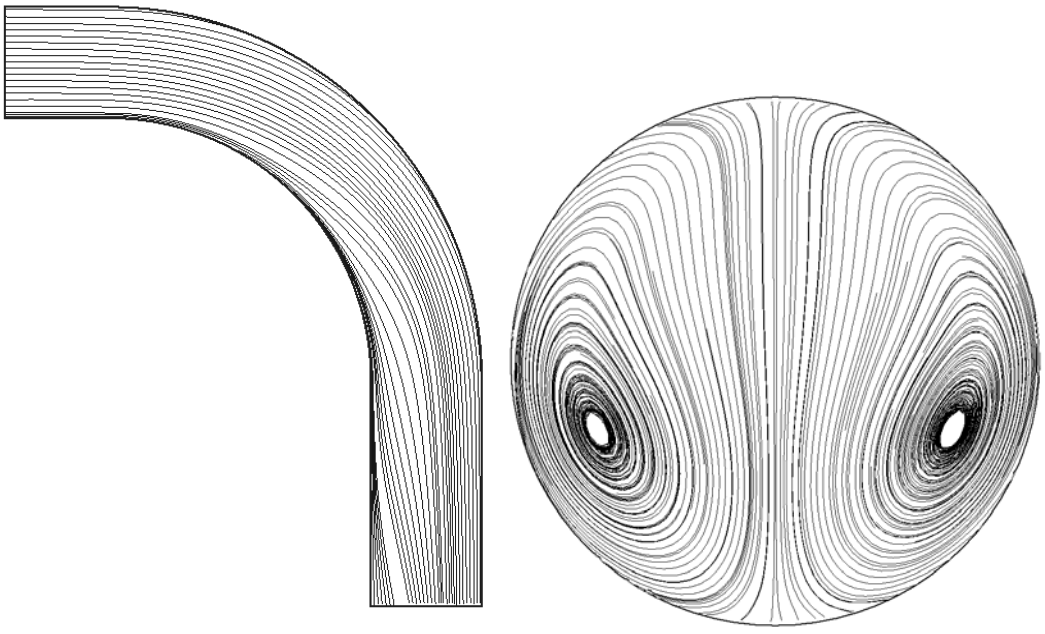

Figure 2: The streamlines of the mean flow in the midplane of the bend and secondary flow in the bend for the deflection angle of 90° at Re = 10000 and De = 4225.

2.3 Aerosol deposition in circular bends

The total process of aerosol deposition can be measured by the penetration of particles which is defined as the ratio of the particle flow rates in the outlet and inlet sections of the bend, $\xi = G_{outlet} / G_{inlet}$, or by the deposition efficiency, $\eta = 1 - \xi$. Fig. 3 presents the deposition efficiency predicted in the 90° bend under the conditions

corresponding to experiment by Pui et al. [16] for Re=10000, De=4225, R_0=5.6, and ρ_p/ρ_f=755. The inertia of particles is quantified by the Stokes number defined as St=$2\tau_p U_m/D$. In these circumstances, the deposition of particles is caused by the simultaneous action of diffusion, turbophoresis, gravity, and centrifugal force. However, the dominating mechanism is the centrifugal force due to the curvature of the main flow and the formation of the secondary flow. As is clear from Fig. 4, the effect of the Stokes number predicted by the DIM is in good agreement with both experimental data [16] and simulations [17, 18].

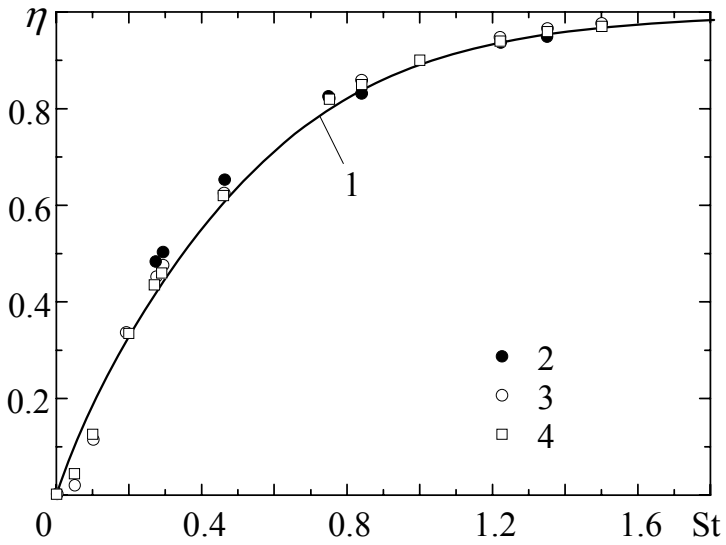

Figure 3: The effect of Stokes number on the deposition efficiency in the 90° bend. (1) DIM, (2) experiment by Pui et al. [16], (3) LES by Breuer et al. [17], (4) LES by Berrouk and Laurence [18].

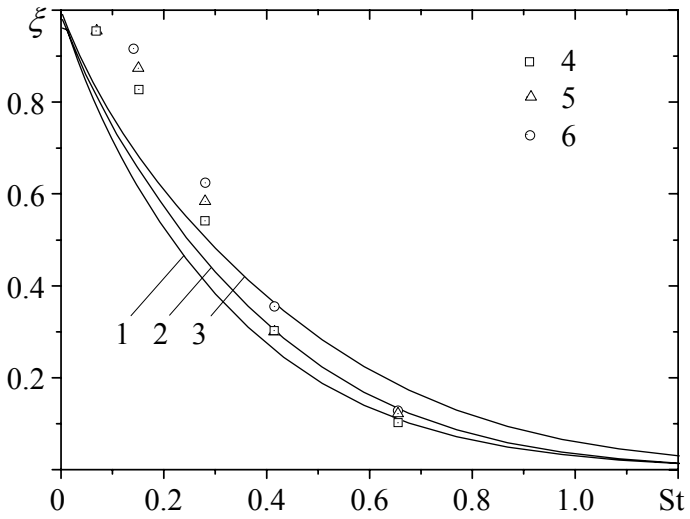

Figure 4: The effects of curvature ratio and Stokes number on the penetration of particles in the 90° bend. (1-3) DIM, (4-6) experiment by McFarland et al. [19]: (1, 4) R_0=4, (2, 5) R_0=10; (3, 6) R_0=20.

Fig. 4 demonstrates the effects of and curvature ratio and Stokes number on the penetration of particles in the 90° bend at Re=10000. Predictions are compared with experiments performed by McFarland et al. [19] in a wide range of curvature ratio. It is

obvious that the centrifugal effect increases as the curvature ratio decreases. Therefore, the penetration falls with both increasing St and decreasing R_0. As is clear, the DIM reasonably reproduces these effects. Some distinction between the predictions and the measurements is observed at small Stokes numbers, when the DIM overestimates the deposition rate.

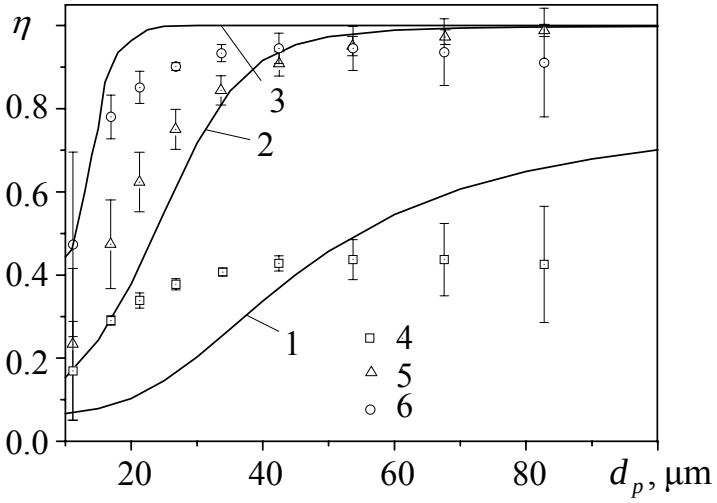

Figure 5: The effects of particle size and bend angle on the deposition efficiency. (1-3) DIM, (4-6) experiment by Peters and Leith [20]: (1, 4) 45°; (2, 5) 90°; (3, 6) 180°.

Fig. 5 compares the deposition efficiency as a function of bend angle with experimental data by Peters and Leith [20] at Re = 203000 and R_0 = 5. These experiments were carried out in bends of D = 0.152 m at a mean velocity of 20 m/s, and hence they were the first to be directly applicable to industrial bends. As is clear from Fig. 5, the deposition efficiency increases for a given particle size. Taking into consideration a great uncertainty of measurements, Fig. 5 indicates that the DIM can reasonably describe the deposition of aerosols at such high Reynolds numbers which are typical of industrial applications.

3 CONCLUSIONS

The model stems from a kinetic equation for the probability density function of velocity distribution of particles whose response times do not exceed the integral timescale of fluid turbulence. The salient feature of the DIM consists in expressing the particle velocity as an expansion in terms of the properties of the carrier fluid, with the particle response time as the small parameter. By this means, the problem of modelling the dispersion of the particulate phase reduces to solving a sole equation for the particle concentration. Thus, computational times are seriously shortened as compared to full two-fluid Eulerian models. The model presented is capable of predicting the main trends of particle distribution including the effect of preferential accumulation due to turbophoresis.

The DIM has been incorporated in a CFD code OpenFOAM and coupled with fluid RANS in the frame of two-way coupling. Simulations of aerosol deposition in straight ducts and circular bends have been performed. The results of deposition efficiency obtained using the DIM are found to be in encouraging agreement with both experimental data and Lagrangian tracking simulations coupled with fluid DNS or LES.

REFERENCES

[1] L.I. Zaichik, A statistical model of particle transport and heat transfer in turbulent shear flows, *Phys. Fluids* **11**, pp. 1521-1534 (1999)

[2] L.I. Zaichik, B. Oesterle, V.M. Alipchenkov, On the probability density function model for the transport of particles in anisotropic turbulent flow, *Phys. Fluids* **16**, pp. 1956-1964 (2004)

[3] L.I. Zaichik, Modelling of the motion of particles in non-uniform turbulent flow using the equation for the probability density function, *J. Appl. Mathematics and Mechanics* **61**, pp. 127-133 (1997)

[4] L.I. Zaichik, V.A. Pershukov, M.V. Kozelev, A.A. Vinberg, Modeling of dynamics, heat transfer, and combustion in two-phase turbulent flows: 1. Isothermal flow, *Exper. Thermal and Fluid Science* **15**, pp. 291-310 (1997)

[5] L.I. Zaichik, V.A. Pershukov, M.V. Kozelev, A.A. Vinberg, Modeling of dynamics, heat transfer, and combustion in two-phase turbulent flows: 2. Flows with heat transfer and combustion, *Exper. Thermal and Fluid Science* **15**, pp. 311-322 (1997)

[6] L.I. Zaichik, S.L. Soloviev, A.P. Skibin, V.M. Alipchenkov, A diffusioñinertia model for predicting dispersion of low-inertia particles in turbulent flows, in: Proceedings of the 5th International Conference on Multiphase Flow, Yokohama, Japan, 2004

[7] L.I. Zaichik, N.I. Drobyshevsky, A.S. Filippov, R.V. Mukin, V.F. Strizhov, A diffusion-inertia model for predicting dispersion and deposition of low-inertia particles in turbulent flows, *Int. J. of Heat and Mass Transfer* **53**, pp. 154-162 (2010)

[8] L.Talbot, R.K. Cheng, R.W. Schefer, D.R. Willis, Thermophoresis of particles in a heated boundary layer, *J. Fluid Mech.* **101**, pp. 737–758 (1980)

[9] B.E. Launder, D.B. Spalding, The numerical computation of turbulent flows, *Comut. Meth. Appl. Mech. Eng.* **3**, pp. 269–289 (1974)

[10] G.A. Kallio, M.W. Reeks, A numerical simulation of particle deposition in turbulent boundary layer, *Int. J. Multiphase Flow* **15**, pp. 433-446 (1989)

[11] J.B. McLaughlin, Aerosol particle deposition in numerically simulated channel flow, *Phys. Fluids A* **1**, pp. 1211–1224 (1989)

[12] B.Y.H. Liu, J.K. Agarwal, Experimental observation of aerosol deposition in turbulent flow, *J. Aerosol Sci.* **5**, pp. 145-155 (1974)

[13] C. Marchioli, A. Giusti, M.V. Salvetti, A. Soldati, Direct numerical simulation of particle wall transfer in upward turbulent pipe flow, *Int. J. Multiphase Flow* **29** ,pp. 1017-1038 (2003)

[14] C. Marchioli, M. Picciotto, A. Soldati, Influence of gravity and lift on particle velocity statistics and transfer rates in turbulent vertical channel flow, *Int. J. Multiphase Flow* **33**, pp. 227-251 (2007)

[15] Q. Wang, K.D. Squires, M. Chen, J.B. McLaughlin, On the role of the lift force in turbulence simulations of particle deposition, *Int. J. Multiphase Flow* **23**, pp. 749–763 (1997)

[16] D.Y.H. Pui, F. Romay-Novas, B.Y.H. Liu, Experimental study of particle deposition in bends of circular cross-section, *Aerosol Sci. and Technol.* **7**, pp. 301-315 (1987)

[17] M. Breuer, H.T. Baytekin, E.A. Matida, Prediction of aerosol deposition in 90^o bends using LES and an efficient Lagrangian tracking method, *J. of Aerosol Science* **37**, pp. 1407-1428 (2006)

[18] A.S. Berrouk, D. Laurence, Stochastic modelling of aerosol deposition for LES of 90^o bend turbulent flow, *Int. J. Heat and Fluid Flow* **29**, pp. 1010-1028 (2008)

[19] A.R. McFarland, H. Gong, A. Muyshondt, W.B. Wente, N.K. Anand, Aerosol deposition in bends with turbulent flow, *Environ. Sci. Technol.* **31**, pp. 3371-3377 (1997)

[20] T.M Peters, D. Leith, Particle deposition in industrial duct bends, *Ann. Occup. Hyg.* **48**, pp. 483-490 (2004)